



UKAEA

Preprint

FOURIER OPTICS APPROACH TO FAR FORWARD  
SCATTERING AND RELATED REFRACTIVE INDEX  
PHENOMENA IN LABORATORY PLASMAS

D. E. EVANS  
M. von HELLERMANN  
E. HOLZHAUER



CULHAM LABORATORY  
Abingdon Oxfordshire

1982

CLM - P 655

This document is intended for publication in a journal or at a conference and is made available on the understanding that extracts or references will not be published prior to publication of the original, without the consent of the authors.

Enquiries about copyright and reproduction should be addressed to the Librarian, UKAEA, Culham Laboratory, Abingdon, Oxon. OX14 3DB, England.

FOURIER OPTICS APPROACH TO FAR FORWARD SCATTERING  
AND RELATED REFRACTIVE INDEX PHENOMENA  
IN LABORATORY PLASMAS

D E Evans, M von Hellermann<sup>1</sup>, and E Holzhauer<sup>2</sup>

Culham Laboratory, Abingdon, Oxon., OX14 3DB, England  
(Euratom/UKAEA Fusion Association)

A B S T R A C T

The transmission of a gaussian beam of electromagnetic radiation through a refracting medium such as plasma, containing within it a localized sinusoidal disturbance, is described entirely in terms of refraction and diffraction. The lowest order terms of an expansion for the intensity profile of a beam in the front focal plane of a lens situated a focal length beyond a beam waist in the medium are identified with well-known optical effects usually treated independently, including shadowgraph, scattering, and schlieren. The latter is shown to be indistinguishable from spontaneous heterodyning of the scattered radiation with the unperturbed beam, and is sensitive to frequency, wavelength, and the location of the disturbance in the medium. An experiment using a HeNe laser and monochromatic ultrasound in atmospheric air has verified the predictions of the model over a wide range of conditions.

As a plasma diagnostic, the method may offer a unique means of measuring otherwise inaccessible very long wavelength instabilities such as trapped ion modes in large tokamaks like JET.

(Accepted for publication in Plasma Physics)

<sup>1</sup> University of Essen, Germany

<sup>2</sup> University of Stuttgart, Germany



## 1. Introduction

A powerful method of measuring turbulence and microinstabilities in fusion research plasmas is collective scattering of laser radiation. Successful studies of this kind have been reported from the ALCATOR tokamak (Slusher and Surko 1980), the WENDELSTEIN stellarator (Meyer and Mahn 1981), and the INTEREX thetapinch (Fahrbach et al 1981), all using CO<sub>2</sub> lasers. Work with FIR lasers has been reported from the MICROTOR tokamak (Semet et al 1980, Park et al 1980).

In the conventional arrangement, the domain of fluctuating wavelength is accessed by using a range of scattering angles and probe beam wavelengths. If long wavelength fluctuations are to be measured, the scattering angles, especially for CO<sub>2</sub> lasers, can become smaller than the beam divergence, and resolution both in k-space and real space becomes very poor (Holzhauer and Massig 1978). Nevertheless experiments have been performed under such conditions, for example by Slusher and Surko (1980) who call it "homodyne" scattering, and by Pots et al (1981) who have referred to "small k" scattering.

The approach described in the present paper is suggested by the observation that any beam of radiation traversing a refracting medium emerges modified in phase and amplitude. It turns out that wavelength, frequency, amplitude, and even location of the phase fluctuations in the medium can be deduced from the emergent beam's wavefront. The analysis is considerably simplified if the incident beam is a coherent gaussian and the phase shifts it encounters are sufficiently small.

In passing through a fluctuating medium the probing beam's intensity profile will have acquired oscillating components, and the amplitude, frequency, and relative phase of these, and their

distribution over the profile constitute the measured data.

Techniques based on refractivity have been used in the past to diagnose turbulence in magnetically confined plasma e.g. Gondhalekar (1968), Robinson and King (1968), Hamberger and Sharp (1976). They are also used in radio astronomy to study interplanetary plasma scintillation e.g. Cohen et al (1967) and a general theory applicable to the latter has been provided by Salpeter (1967) and Lovelace et al (1970).

The method is also known to electrical engineers involved in acousto-optic signal processing methods e.g. Korpel(1972, 1981), Rhodes (1981).

Section 2 of this paper outlines the theory pertinent to our case, developed on the assumption of a monochromatic disturbance in the plasma, which could be one Fourier component of more general turbulence. It leads to an equation for the intensity distribution of the beam in the front focal plane of a lens placed a focal length beyond a gaussian beam waist within the medium under investigation. Sections 3 and 4 describe the time-independent and the lowest order time-dependent terms of the intensity distribution. The dependence of the latter on  $z$ , the measure of position along the beam axis, is also discussed. A feature of the method is its capacity to locate long wavelength fluctuations using a single probe beam, and it therefore offers an alternative to the crossed beam correlation technique used by Surko and Slusher (1980).

Section 5 deals with the time-dependent second order term. Experiments lending strong support to the calculations are described briefly in Section 6.

## 2. Theory

The propagation of a beam of radiation can be entirely described by diffraction, and its interaction with the intervening matter by refraction.

Let radiation travel in the +z direction, and let its amplitude distribution in any plane to which the z-axis is normal be U. Let z be measured from the left hand, or back, focal plane of a lens of focal length f lying in the  $(x_l, y_l)$  plane, as illustrated in Figure 1.

According to Huygens-Fresnel diffraction theory (Goodman, 1968) the amplitude distribution  $U(x, y)$  at a plane a distance z from the lens's back focal plane, and the distribution  $U(x_l, y_l)$  at the lens plane are related by the integral equation

$$U(x_l, y_l) = \iint_{-\infty}^{\infty} h(x_l, y_l, x, y) U(x, y) dx dy \quad \dots(1)$$

where, in the Fresnel approximation, the kernel  $h(x_l, y_l, x, y)$

is given by

$$h = \frac{e^{i \frac{2\pi}{\lambda}(f-z)}}{i \lambda (f-z)} e^{i \frac{\pi}{\lambda(f-z)} [(x_l - x)^2 + (y_l - y)^2]},$$

$\lambda$  being the wavelength of the radiation.

The effect of passing through the lens is represented by multiplying  $U(x_l, y_l)$  by the phase factor

$$e^{-i \frac{\pi}{\lambda f} (x_l^2 + y_l^2)}$$

Projecting to the front focal plane of the lens by a second application of the diffraction integral results in the amplitude

$$U(x_f, y_f) = \iint_{-\infty}^{\infty} h(x_f, y_f, x_l, y_l) U(x_l, y_l) e^{-i \frac{\pi}{\lambda f} (x_l^2 + y_l^2)} dx_l dy_l$$

$$\text{with } h(x_f, y_f, x_l, y_l) = \frac{e^{i \frac{2\pi f}{\lambda}}}{i \lambda f} e^{i \frac{\pi}{\lambda f} [(x_f - x_l)^2 + (y_f - y_l)^2]}.$$

After some manipulation,  $U(x_f, y_f)$  reduces to

$$U(x_f, y_f) = \frac{e^{i \frac{4\pi f}{\lambda}}}{i \lambda f} e^{-i \frac{2\pi z}{\lambda} (1 - \frac{x_f^2 + y_f^2}{2f^2})} \iint_{-\infty}^{\infty} U(x, y) e^{-i \frac{2\pi}{\lambda f} (xx_f + yy_f)} dx dy, \quad \dots (2)$$

where  $\frac{2\pi x_f}{\lambda f} \equiv K_x$  plays the role of a spatial wavenumber in the  $(x, y)$  plane.

We now consider a particular experimental arrangement, illustrated in Figure 2, where the amplitude distribution  $U(x, y)$  is taken to be that of a gaussian beam a distance  $z$  beyond its beam waist, say  $U_g(x, y)$ , modified by a phase



factor  $e^{i\varphi(x,y)}$ . The gaussian amplitude distribution can be represented by (Siegman, 1971)

$$U_g(x,y) = \frac{1}{\sqrt{\pi} W} e^{-i\left(\frac{2\pi z}{\lambda} - \phi(z)\right) - (x^2 + y^2) Q^2} \dots(3)$$

Here,  $Q^2 \equiv (1/2W^2)(1+i\frac{z}{z_r})$ ,  $W$  being the beam width parameter at  $z$ , defined so that the half-width of the intensity profile at the  $1/e$  height is  $W$ . At the beam waist, where  $z=0$ ,  $W$  becomes  $W_0$ . The parameter  $z_r \equiv \frac{2\pi W_0^2}{\lambda}$ , the Rayleigh zone, and  $\phi(z)$  is a phase factor independent of distance transverse the  $z$ -axis.

It can be seen that  $U_g(x,y)$  describes constant phase surfaces, i.e. wavefronts, that are curved, except at the beam waist ( $z=0$ ) where they become plane. For the phase factor we adopt a monochromatic oscillation, wavenumber  $K$ , frequency  $\Omega$ , varying only in the  $x$ -direction, which we write

$$\varphi(x,y) = \Delta\varphi \sin(Kx - \Omega t), \dots(4)$$

$\Delta\varphi$  being related to the refractive index of the medium at  $z$  by

$$\Delta\varphi = 2\pi \frac{L}{\lambda} \Delta\mu$$

where  $L$  is the length along the  $z$ -axis over which this phase grating interacts with the beam of radiation.

Localizing the disturbance in the form of a phase grating at the axial position  $z$  in this way amounts to adopting a Raman-Nath rather than a Bragg model for the interaction. This is justified by the fact that the Klein-Cook parameter  $\frac{\lambda L K^2}{2\pi}$  (Klein and Cook 1967) can be assumed to be  $\ll 1$  in all that follows.

In un-ionised gas the phase factor becomes

$$\Delta\varphi = \frac{2\pi L}{\lambda} (\mu_0 - 1) \frac{\Delta p}{p_0} \quad \dots(5)$$

where  $\Delta p/p_0$  is the fractional pressure change and  $\mu_0$  is the gas index of refraction. For plasma  $\mu^2 = 1 - \omega_{pe}^2/\omega^2$ ,  $\omega_{pe}$  being the electron plasma angular frequency, and accordingly

$$\Delta\varphi = r_e \lambda L \Delta n_e. \quad \dots(6)$$

Here,  $r_e$  is the electron radius and  $n_e$  the electron density.

We accordingly substitute  $U(x,y) = U_g(x,y)e^{i \Delta\varphi \sin(Kx - \Omega t)}$  into equation (2) and perform the integration to obtain the amplitude distribution  $U(x_f, y_f)$  in the front focal plane. To facilitate the integration, the phase factor is expanded in a Bessel function series

$$e^{i \Delta\varphi \sin(Kx - \Omega t)} = \sum_{l=-\infty}^{+\infty} J_l(\Delta\varphi) e^{i l(Kx - \Omega t)} ;$$

use is made of two relations from gaussian optics, viz.

$$W_f W_0 = \frac{\lambda f}{2\pi} \quad \text{and} \quad W = W_0 \sqrt{[1 + (z/z_r)^2]} ,$$

$x_f$  is normalised to the spot size  $W_f$  in the front focal plane:

$$u \equiv x_f/W_f ,$$

and finally, the dimensionless parameter  $v$  relating the spot size at the beam waist  $W_0$  in the refractive medium to the wavenumber  $K$  of the phase modulation, is introduced:

$$v \equiv K W_0 . \quad \dots(7)$$

The amplitude in the front focal plane is then found to be

$$U(u, y_f) = e^{i(\text{real})} \frac{2\sqrt{\pi} W_0 (1 - iz/z_r) e^{-\frac{1}{2}(y_f/W_f)^2}}{i \lambda f \sqrt{[1 + (z/z_r)^2]}} \\ \times \sum_{\ell=-\infty}^{\infty} J_{\ell}(\Delta\varphi) e^{-\frac{1}{2}(u-\ell v)^2} e^{i[\frac{1}{2}(z/z_r)(u-\ell v)^2 - \ell\Omega t]} .$$

This is multiplied by its complex conjugate to produce the expression for the intensity distribution in this plane.

As we envisage viewing through a slit parallel to the wave fronts of the phase modulation, that is, parallel to the  $y_f$  direction, the integral along this direction is also performed. The resulting intensity distribution is

$$I(u) = |U(u)|^2 \\ = \frac{1}{\sqrt{\pi} W_f} \left\{ (\sum J_{\ell}(\Delta\varphi) e^{-\frac{1}{2}(u-\ell v)^2} \cos[\frac{1}{2}(z/z_r)(u-\ell v)^2 - \ell\Omega t])^2 \right. \\ \left. + (\sum J_{\ell}(\Delta\varphi) e^{-\frac{1}{2}(u-\ell v)^2} \sin[\frac{1}{2}(z/z_r)(u-\ell v)^2 - \ell\Omega t])^2 \right\} .$$

The Bessel functions are replaced by their small argument approximations

$$J_0(\Delta\varphi) \approx 1 - \frac{1}{4}(\Delta\varphi)^2, \quad J_{\ell}(\Delta\varphi) \approx \left(\frac{1}{2}\Delta\varphi\right)^{\ell} \frac{1}{\ell!}, \quad \text{where } J_{-\ell} = (-1)^{\ell} J_{\ell};$$

and terms in  $\Delta\varphi$  of order greater than 2 are discarded. The outcome of this procedure is the following expression for the intensity distribution in the front focal plane.

$$\begin{aligned}
I(u) = \frac{I_0}{\sqrt{\pi} W_f} & \left\{ e^{-u^2} \left[ 1 - \frac{1}{2} (\Delta\varphi)^2 \right] \right. \\
& + \Delta\varphi e^{-\left(\frac{1}{2}v\right)^2} \left[ e^{-\left(u-\frac{1}{2}v\right)^2} \cos\left[\frac{z}{z_r} v\left(u-\frac{1}{2}v\right) + \Omega t\right] \right. \\
& \quad \left. \left. - e^{-\left(u+\frac{1}{2}v\right)^2} \cos\left[\frac{z}{z_r} v\left(u+\frac{1}{2}v\right) + \Omega t\right] \right] \right. \\
& + \left(\frac{1}{2}\Delta\varphi\right)^2 \left[ e^{-\left(u-v\right)^2} + e^{-\left(u+v\right)^2} \right] \\
& + \left(\frac{1}{2}\Delta\varphi\right)^2 e^{-v^2} \left[ e^{-\left(u-v\right)^2} \cos\left[2\Omega t + 2\frac{z}{z_r} v\left(u-v\right)\right] \right. \\
& \quad \left. + e^{-\left(u+v\right)^2} \cos\left[2\Omega t + 2\frac{z}{z_r} v\left(u+v\right)\right] \right. \\
& \quad \left. - 2e^{-u^2} \cos\left[2\Omega t + 2\frac{z}{z_r} uv\right] \right] \left. \right\} \dots(8)
\end{aligned}$$

When the phase disturbance is located at the beam waist,  $z = 0$ , the spatial profile and the time dependence can be separated. Figure 3 shows  $z = 0$  spatial profiles of the leading terms for four values of the parameter  $v$ .

### 3. Time Independent Terms

The first time-independent term,  $J_0(\Delta\varphi) e^{-u^2}$  without approximation, describes the undeviated but slightly attenuated transmitted beam. It has a gaussian profile with a half-width  $W_f$  conjugate to the half-width  $W_0$  of the beam waist at the back focal plane. The small attenuation can be understood as the loss to the main beam of radiation that appears displaced from it in the higher order terms, the most prominent of these being the second time-independent term.

The latter is proportional to  $\left(\frac{1}{2}\Delta\varphi\right)^2$  and is accordingly very much less intense than the undeviated beam. It is also

independent of the axial location  $z$ . When the refracting medium is plasma,

$$\left(\frac{1}{2}\Delta\phi\right)^2 = \frac{1}{4} r_e^2 \lambda^2 L^2 (\Delta n_e)^2 ,$$

which can be recognised as the Thomson scattering of a gaussian beam from a monochromatic electron density wave. The spatial profile of this term consists of two gaussian maxima disposed symmetrically on either side of the origin, centred at  $u = \pm v$  respectively, and each with the same width,  $W_f$ , as the undeviated beam spot.

The equation  $u = v$  can readily be shown to be equivalent to the Bragg relation,  $K = 4\pi \lambda^{-1} \sin \theta/2$ , for small scattering angle  $\theta$ . Moreover, if  $W_f$  is regarded as a measure of the uncertainty in the exact position  $x_f$  of the maxima, viz  $\Delta x_f = W_f$ , then from equation (2),  $K/\Delta K = \frac{K \lambda f}{2\pi \Delta x_f} = \frac{K \lambda f}{2\pi W_f} = K W_0 = v$ . That is to say, the parameter  $v$  can be seen to be a measure of the resolution in wavenumber  $K$ , and is essentially the  $K$ -resolution parameter called "r" in Holzhauser and Massig (1978).

#### 4. First Order Time Dependent Term

The term proportional to  $\Delta\phi$  oscillates at the frequency  $\Omega$  of the phase wave and is accordingly easy to distinguish experimentally from the time-independent terms. Unlike them, it is also a function of axial position  $z$ .

Fluctuations at the beam waist where  $z=0$ , have a profile

$$\Delta\phi \cos \Omega t e^{-\left(\frac{1}{2}v\right)^2} \left[ e^{-\left(u-\frac{1}{2}v\right)^2} - e^{-\left(u+\frac{1}{2}v\right)^2} \right], \quad \dots(9)$$

which is the difference of two gaussians centred at  $u = \pm \frac{1}{2}v$

and is evidently antisymmetric with respect to the origin. The profile maxima almost coincide with those of the gaussians when  $v \geq 2$ , and when  $v$  approaches 0, the profile maxima approach  $\pm 1/\sqrt{2}$ . Thus the accurate location of these maxima, for example by a process of curve fitting, permits the wavenumber  $K$  to be determined to arbitrary accuracy, at least in principle.

Figure 4 plots the strength of these maxima as a function of  $v$ . They are most pronounced near  $v=1$ , that is, when the wavelength of the phase disturbance is about three times the beam waist spot size. They diminish rapidly when  $v$  is much larger or smaller than unity.

The antisymmetric and oscillatory character of this term, as well as its dependence on the first power of  $\Delta\phi$  invites its identification as a refraction or schlieren phenomenon. That is, the antisymmetric oscillations could be interpreted as the result of the phase wave passing across the radiation beam and deflecting it to and fro, resulting in the oscillation of the spot in the front focal plane of the lens as diagrammed in Figure 5.

Further insight into the nature of this first order term is gained by noticing that it could have been generated by the Thomson scattering terms

$$\left(\frac{1}{2}\Delta\phi\right)^2 e^{-u-v} \quad \text{and} \quad \left(\frac{1}{2}\Delta\phi\right)^2 e^{-(u+v)}$$

beating or heterodyning with the term describing the unperturbed beam,  $e^{-u}$ , which then plays the role of a local oscillator. In fact, this heterodyne term, which appears spontaneously in our analysis, is the one already familiar as "homodyne detection" in Slusher and Surko (1980).

When dependence on axial position  $z$  of the phase disturbance

relative to the beam waist is retained in the first order time-dependent term, the latter continues to describe the difference of two gaussians, oscillating at frequency  $\Omega$ , but now out of phase with a phase difference which depends directly on  $z$ . Accordingly, appropriate phase sensitive techniques should allow signals originating local to a predetermined  $z$  to be discriminated and selectively measured.

To emphasise and illustrate the  $z$ -dependent behaviour of the first order time-dependent term, we separate it into the sum of its odd and even parts:

$$I = \Delta\varphi e^{-\left(\frac{1}{2}v\right)^2} \left[ e^{-A_-^2} \cos\left(\frac{z}{z_r} vA_- + \Omega t\right) - e^{-A_+^2} \cos\left(\frac{z}{z_r} vA_+ + \Omega t\right) \right] \dots(10)$$

=  $I_{\text{even}} + I_{\text{odd}}$ , where

$$I_{\text{even}} = \frac{I(u) + I(-u)}{2}$$

$$= \Delta\varphi e^{-\left(\frac{1}{2}v\right)^2} \left[ e^{-A_+^2} \sin \frac{z}{z_r} vA_+ - e^{-A_-^2} \sin \frac{z}{z_r} vA_- \right] \sin \Omega t$$

... (11)

$$I_{\text{odd}} = \frac{I(u) - I(-u)}{2}$$

$$= \Delta\varphi e^{-\left(\frac{1}{2}v\right)^2} \left[ e^{-A_-^2} \cos \frac{z}{z_r} vA_- - e^{-A_+^2} \cos \frac{z}{z_r} vA_+ \right] \cos \Omega t$$

... (12)

where  $A_{\pm} = u \pm \frac{1}{2}v$ .

$I_{\text{even}}$  and  $I_{\text{odd}}$  can be constructed in a practical experiment by adding and subtracting the positive and negative sides of the real time recorded profile  $I(u,t)$ . Curve fitting can then be used to extract the values of  $z$ ,  $v$ , and  $\Delta\varphi$ .

$I_{\text{even}} = 0$  when  $z = 0$ , and varies rapidly as  $z$  increases.  $I_{\text{odd}}$  is sensitive to the direction of the phase wave in that a change from  $K$  to  $-K$  alters  $I_{\text{odd}}$  to  $-I_{\text{odd}}$ .

The functions  $I_{\text{even}}(u)$  and  $I_{\text{odd}}(u)$  are shown plotted for  $v = 1.5$  and a selection of values of  $z/z_r$  ranging from 0 to 3.6 in Figure 6. The spatial frequency of these functions' structures increases with  $z/z_r$  and the precise profiles are uniquely determined by the pair of parameters  $(z, v)$ . The intensities of  $I_{\text{even}}$  and  $I_{\text{odd}}$ , as opposed to their detailed structure, depend on  $v$  and  $\Delta\phi$ , but not on  $z$ .

Sets of functions of this kind could serve as reference curves for the analysis of profiles measured by detector arrays. The measured data would be cross-correlated with the calculated curves for a range of  $z$  values, and the location of a plasma disturbance would be indicated by a high value of the cross-correlation coefficient. A strong maximum would signal a highly localized disturbance, while a plateau would correspond to a broad band of fluctuation.

The axial resolution or "depth of focus" that could be realized by this technique would not be limited to the Rayleigh zone  $z_r$ , but would be determined ultimately by the number of resolved elements and the experimental signal-to-noise ratio. Such a correlation approach and its similarity to synthetic aperture synthesis is discussed by Leith (1978).



## 5. Second Order Time Dependent Term

Because the second order time dependent term in equation (8) is proportional to  $(\Delta\varphi)^2$  and oscillates at  $2\Omega$ , twice the frequency of the plasma disturbance, it is suggestive to identify it with the shadowgraph effect already familiar in plasma diagnostics. It is well known that a dispersive medium, the second derivative of whose index of refraction  $\mu$  is non-vanishing, behaves like a lens with a focal length

$$f_p = \frac{\mu}{\frac{d^2 \mu}{dx^2}},$$

$L$  being the interaction length. For a medium with the sinusoidal phase fluctuation we have assumed throughout, and using

$$\varphi = \frac{2\pi L (\mu - 1)}{\lambda}$$

we find  $f_p^{-1} = \frac{K^2 \lambda}{2\pi} \Delta\varphi \sin(Kx - \Omega t)$ .

The result of adding this fictitious lens to the real focusing lens is to shift the effective position of the beam waist in the medium relative to the real lens, thus moving the waist outside away from the front focal plane, broadening the spot in that plane, so reducing the central intensity, and increasing the intensity far out in the wings. One period of the sinusoidal disturbance in the medium crossing the optical axis can be seen to correspond to two periods of intensity change, which means that the intensity oscillates at twice the frequency of the phase wave.

The size of the intensity oscillation produced in this way can be shown to be

$$\Delta I/I \sim \frac{1}{2}(z_r f_p^{-1})^2 \sim (\Delta\phi)^2 ,$$

while its distribution across the profile, given by the derivative of the gaussian with respect to the spot size, is strikingly similar to the symmetric profiles predicted for the second order time-dependent term, shown in Figure 3 .

So the  $(\Delta\phi)^2$  dependence, the second harmonic frequency, and the spot profile of this term are all consistent with its interpretation as a generalised shadowgraph effect.

## 6. Experimental Verification

Figure 7 is a schematic of an experimental assembly in which the conditions described in the foregoing theory were satisfied as closely as possible. A HeNe laser beam was focused to a waist having  $W_0 = 10^{-2}$  cm and monochromatic, plane, ultrasonic waves at frequencies from  $10^5$  to  $3 \times 10^6$  Hz were launched transverse to the beam axis by a 1 inch piezoelectric crystal in atmospheric air. The crystal could be translated parallel to the beam from the waist to a point 40 cm distant, thus covering four Rayleigh zones,  $z_r$  being 9.9 cm . The intensity profile in the front focal plane of a lens was swept across a slit by means of a vibrating mirror and the resulting photodiode signal was divided and fed to a pair of lock-in amplifiers referred to the frequency of the signal generator that powered the piezoelectric crystal, and mutually separated in phase from each other by  $90^\circ$ .

Traces made in the way described for various positions  $z/z_r$  of the transducer are displayed in Figure 8. The wave frequency was 1 MHz, corresponding to a wavelength in air of 0.3 mm. The left hand traces are the integrated lock-in output for  $I_{\text{even}}$ ; the right hand ones are  $I_{\text{odd}}$ . Comparison with Figure 6 demonstrates that these experimental curves reproduce the corresponding computed profiles in surprising detail. It can be seen that as the value of  $z/z_r$  increases from 0 to 4, the profile shapes alter dramatically. The effect is particularly marked for  $I_{\text{even}}$  for  $z/z_r$  between 0 and 1; over the same range the change in  $I_{\text{odd}}$  is only slight. So  $I_{\text{even}}$  is the best indicator of the location of activity in the medium over this range.

Surko and Slusher (1980) remark that in their correlation experiments, the failure of their homodyne signals to approach zero at the centre of the laser beam profile is not fully understood. Our analysis permits us to explain their discrepancy in terms of plasma fluctuations located away from the laser beam waist.

## 7. Summary and Conclusions

We have discussed the transmission of a gaussian beam of radiation through a refractive medium, such as a plasma, exclusively in terms of refraction and diffraction. The effect of phase fluctuations upon the resulting intensity in the front focal plane of a lens located a focal length beyond a beam waist in the medium was investigated, and for simplicity of interpretation attention was confined to a single sinusoidal mode of the fluctuation travelling transverse to the beam direction.

We find that the lowest order members of an expansion for the intensity profile in terms of phase shift  $\Delta\phi$  can be identified with various well-known optical phenomena usually

thought of as independent. Thus, the second order time-independent term describes scattered radiation satisfying the Bragg condition (which arises naturally out of the theory) and which can be seen to correspond to Thomson scattering when the medium is plasma. The first order time-dependent term appears to describe beam deflection or schlieren, but closer enquiry reveals that it can equally and more profitably be thought of as spontaneous heterodyning of the scattered radiation with the unperturbed part of the beam acting as local oscillator. A second order time-dependent term, oscillating at twice the frequency of the mode in the medium is evidently a generalisation of the well-known shadowgraph effect.

Apart from the unperturbed continuous beam, the self-heterodyning term is the most easily measured since it is comparatively large, being proportional to the first power of  $\Delta\phi$ , and readily discriminated from the unperturbed beam, since it oscillates at the frequency  $\Omega$  of the phase wave in the medium.

One of its most striking features is the sensitivity of its profile to the spatial location along the beam of the wave in the medium. This profile consists of two gaussian maxima spaced symmetrically on either side of the axis, oscillating out of phase with each other at the wave frequency  $\Omega$ . The location along the beam of the wave in the medium manifests itself in the phase difference between the two oscillating gaussians, which reaches its maximum of  $180^\circ$  when the wave is at the beam waist. Accordingly, appropriate phase sensitive detection would focus on a particular location somewhere along the beam, and would record preferentially fluctuations from that location

and discriminate against all others. The method is therefore inherently capable of locating fluctuations without recourse to crossed beams. Indeed, the present analysis suggests that crossed beam data is subject to contamination by fluctuations induced by long wavelength turbulence on the local oscillator beam alone.

The depth of focus, or along-the-beam resolution that could be realized in practice is not limited to the Rayleigh zone  $z_r$ , but must be determined ultimately only by the statistical noise on real observations.

An experiment in which the conditions prescribed by our theory have been met as closely as possible has been assembled using a HeNe laser and near monochromatic ultrasound generated by a small piezoelectric transducer in atmospheric air. The profile of the self-heterodyne term has been analysed into even and odd parts in order to reveal phase information, and the detailed form of these has been measured for a range of fluctuation wavelengths and positions along the laser beam. Predictions of the theory have been verified in every particular over the range of conditions we were able to examine.

Our technique makes it possible to investigate turbulence wavelengths longer than any that could be studied by conventional scattering. It may accordingly be of particular importance in large tokamaks like JET where for example trapped ion mode instabilities having transverse wavelength 6-12 cm may be inaccessible by any other means.

## References

- Cohen M.H. Gundermann E.J. Hardebeck H.E. and Sharp L.E.  
(1967) *Astrophys Journ* 147 449
- Fahrbach H.U. Koppendorfer W. Munich M. Neuhauser J.  
Rohr H. Schram G. Sommer J. and Holzhauser E.  
(1981) *Nucl Fusion* 21 257
- Gondhalekar A.M. (1968) Ph D Thesis, Univ of Manchester
- Goodman J.W. (1968) *Introduction to Fourier Optics*  
pub McGraw-Hill
- Hamberger S.M. Sharp L.E. Lister J.B. and Mrowka S.  
(1976) *Phys Rev Letters* 37 1345
- Holzhauser E. and Massig J.H. (1978) *Plasma Physics* 20 867
- Klein W.R. and Cook W.D. (1967) *IEEE Trans on Sonics*  
and *Ultrasonics* SU-14 123
- Korpel A. Kessler L.W. and Ahmed M. (1972)  
*Journal of the Acoustical Soc Amer* 51 1582
- Korpel A. (1981) *Proc IEEE* 69 48
- Leith E.N. (1978) *Optical Data Processing*  
ed. D. Casasent pub Springer Verlag
- Lovelace R.V.E. Salpeter E.E. Sharp L.E. and Harris D.E.  
(1970) *Astrophys Journ* 159 1047
- Meyer J. and Mahn C. (1981) *Phys Rev Letters* 46 1206
- Park H. Peebles W.A. Mase A. Luhmann N.C. and Semet A.  
(1980) *Applied Physics Letters* 37 279
- Pots B.F.M. Coumans J.J.H. Schram D.C.  
(1981) *Physics of Fluids* 24 517
- Rhodes W.T. (1981) *Proc IEEE* 69 65
- Robinson D.C. and King R.E. (1968) *Proc of IAEA Novosibirsk*  
*Conference on Plasma Physics and Controlled Nuclear*  
*Fusion Research* Vol I 263
- Salpeter E.E. (1967) *Astrophys Journ* 147 433
- Semet A. Mase A. Peebles W.A. Luhmann N.C. and Zweben S.  
(1980) *Phys Rev Letters* 45 445

Siegman A.E. (1971) An Introduction to Lasers and Masers  
pub McGraw-Hill

Slusher R.E. and Surko C.M. (1980) Physics of Fluids 23 472

Surko C.M. and Slusher R.E. (1980) Physics of Fluids 23 2425

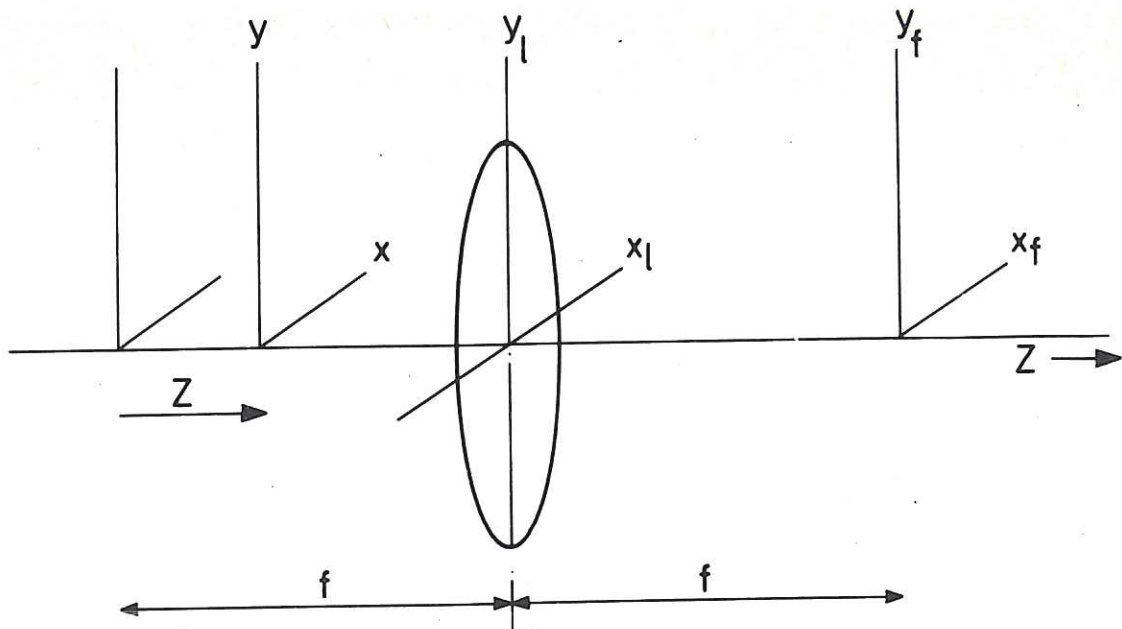
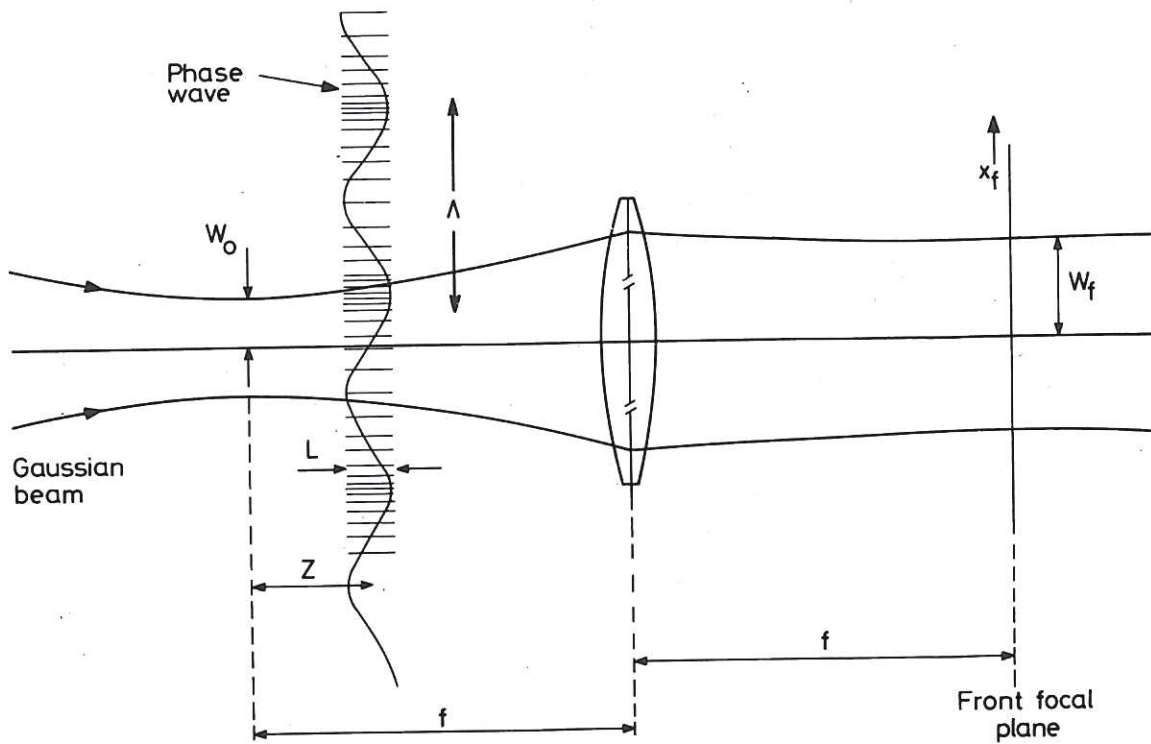


Fig.1 Geometry for Fresnel Diffraction calculation. A lens, focal length  $f$ , is located in the  $x_l, y_l$  plane. Radiation proceeds from left to right along the  $z$ -axis.



— Refractive medium —

Fig.2 Experimental arrangement under analysis. A gaussian beam of radiation, beam waist  $W_0$  at the back focal plane of a lens, focal length  $f$ , proceeds from left to right and encounters a monochromatic phase wave, width  $L$ , wavelength  $\lambda$ , a distance  $z$  to the right of the beam waist. The intensity distribution in the front focal plane is calculated.



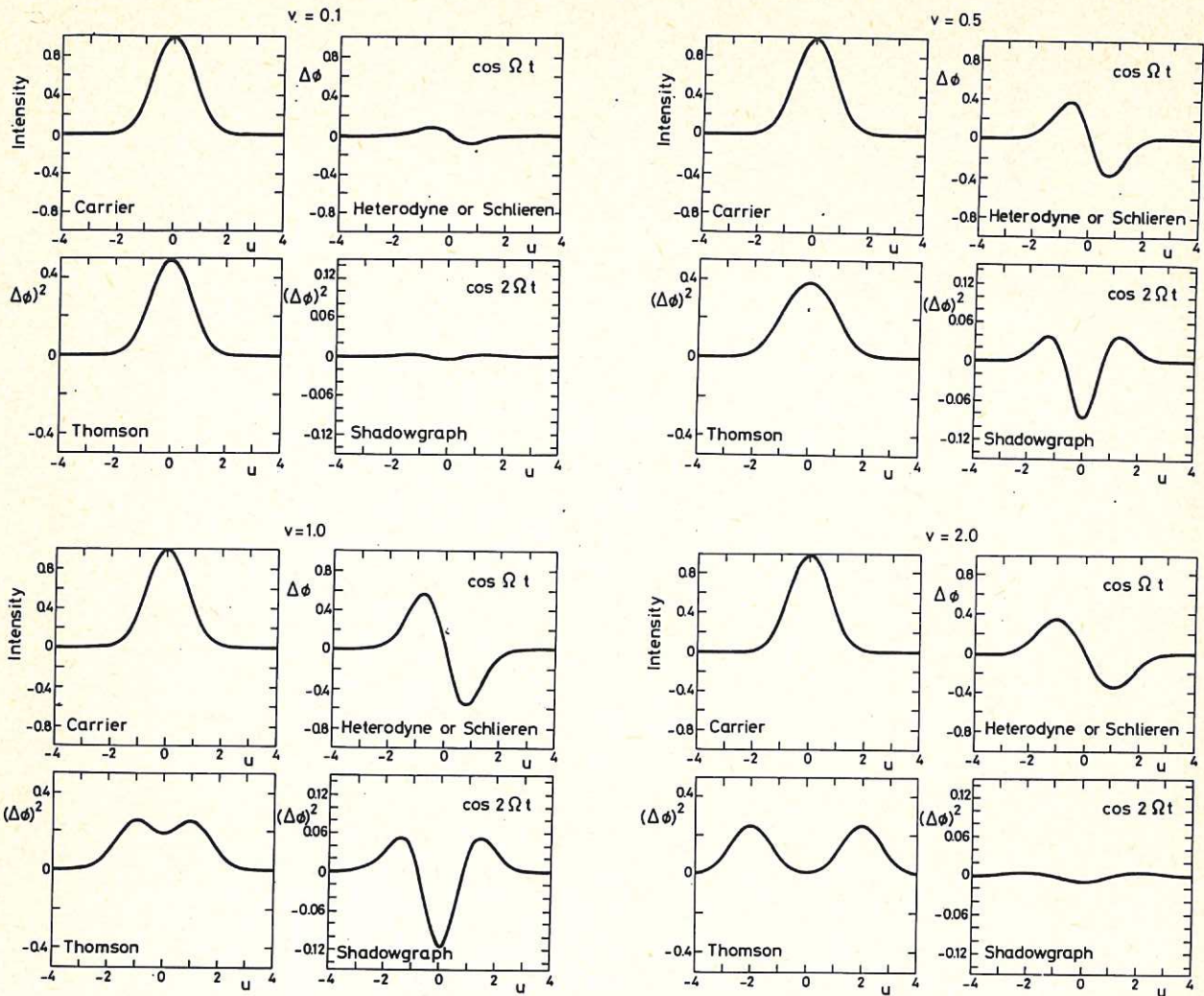


**Fig.3** Normalised spatial profiles of the time-independent (to the left) and time-dependent (to the right) terms to second order in  $\Delta\phi$ . Phase disturbance located in the  $z=0$  plane. The self-heterodyne term arises from the beating of the Thomson scattered and the carrier terms.

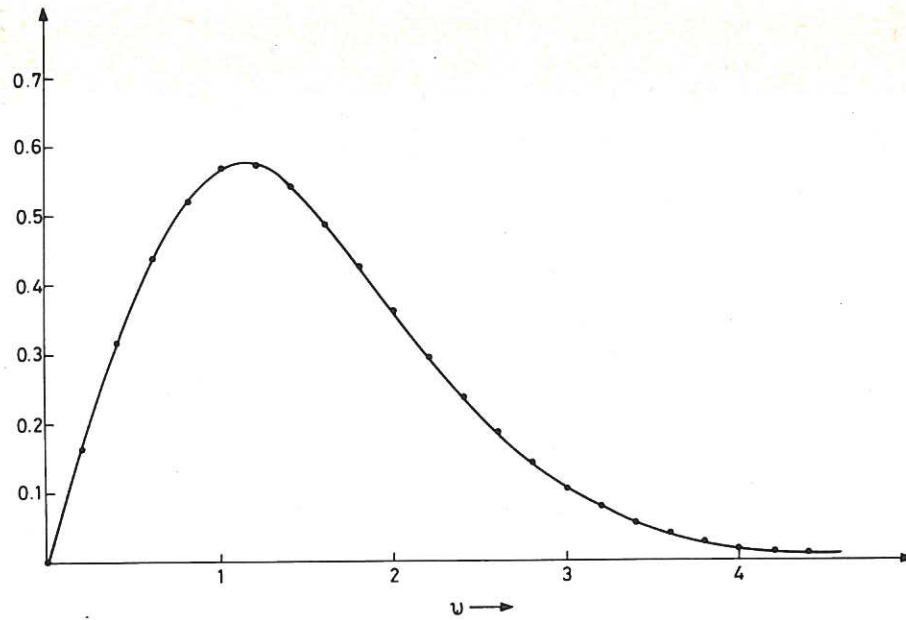


Fig.4 Intensity of the peak of the self-heterodyne term as a function of  $KW_0 \equiv v$ .

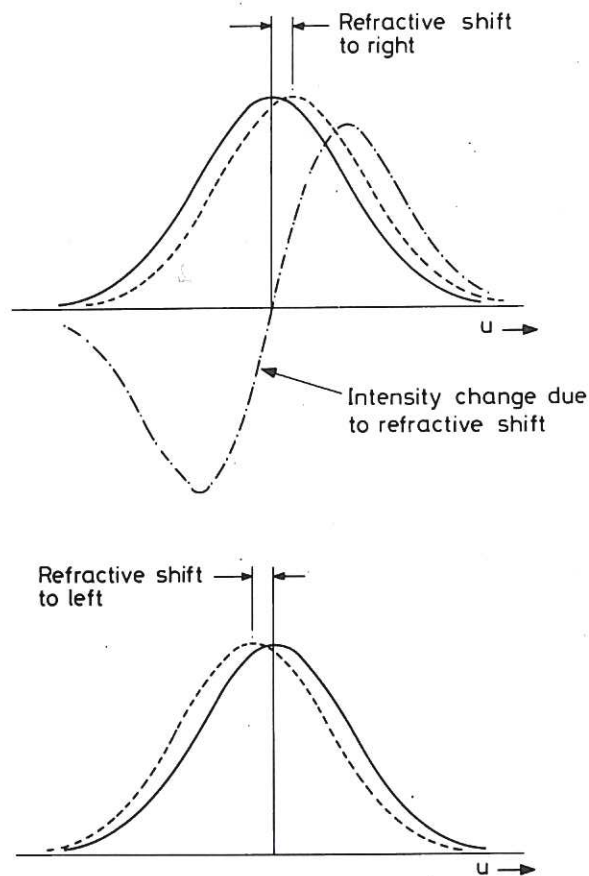


Fig.5 Schlieren interpretation of first order time-dependent term. Gaussian spot in front focal plane of lens shifted slightly to left and to right by simple refraction as phase wave moves across beam in back focal plane, leads to antisymmetric intensity changes in the wings.

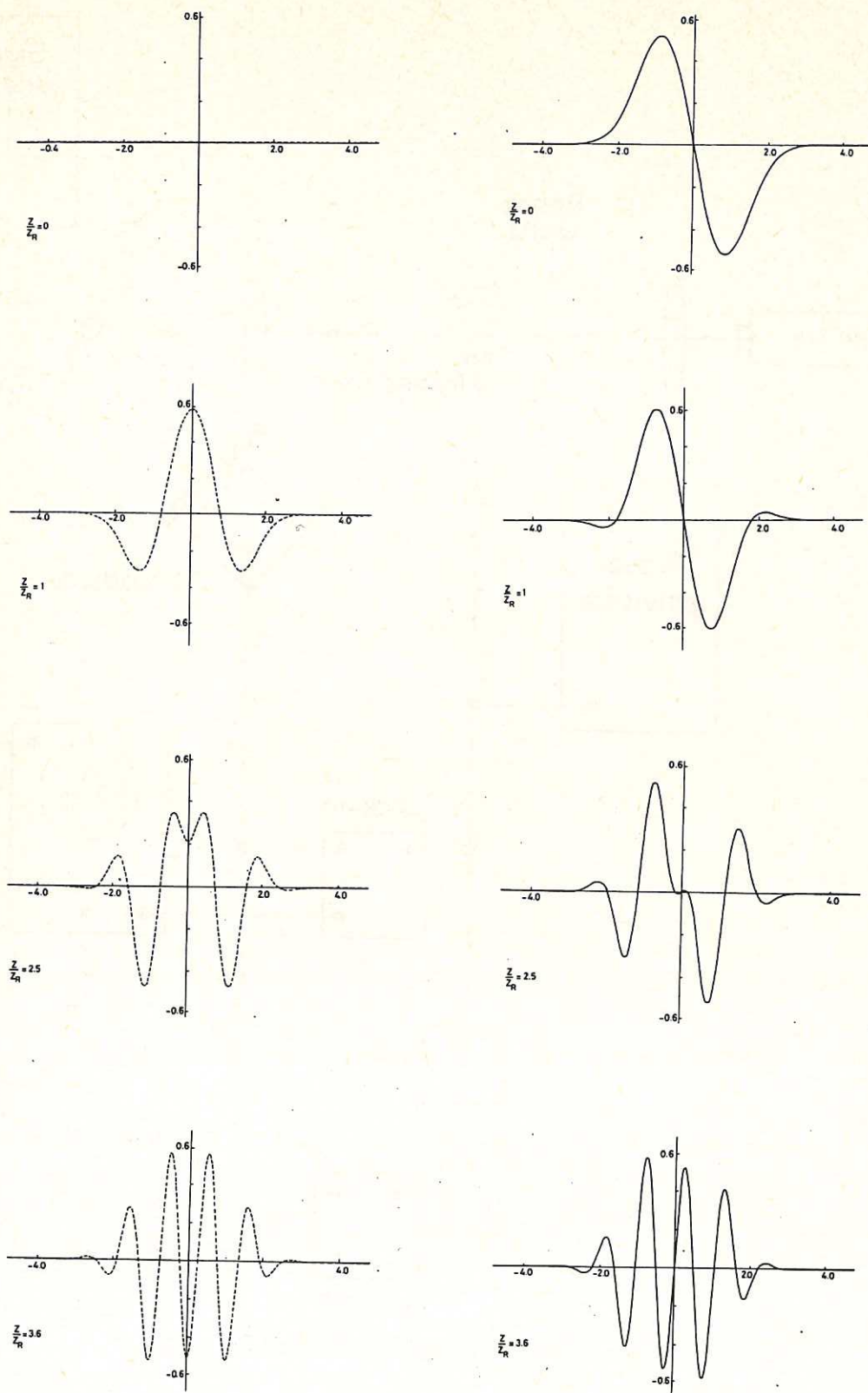


Fig.6 The function  $I_{\text{even}}(u)$  and  $I_{\text{odd}}(u)$  for  $v = 1.5$ , plotted for four different locations  $z/z_T$  of the phase wave relative to the lens back focal plane. The comparative sensitivity of  $I_{\text{even}}$  to  $z/z_T$  is apparent.

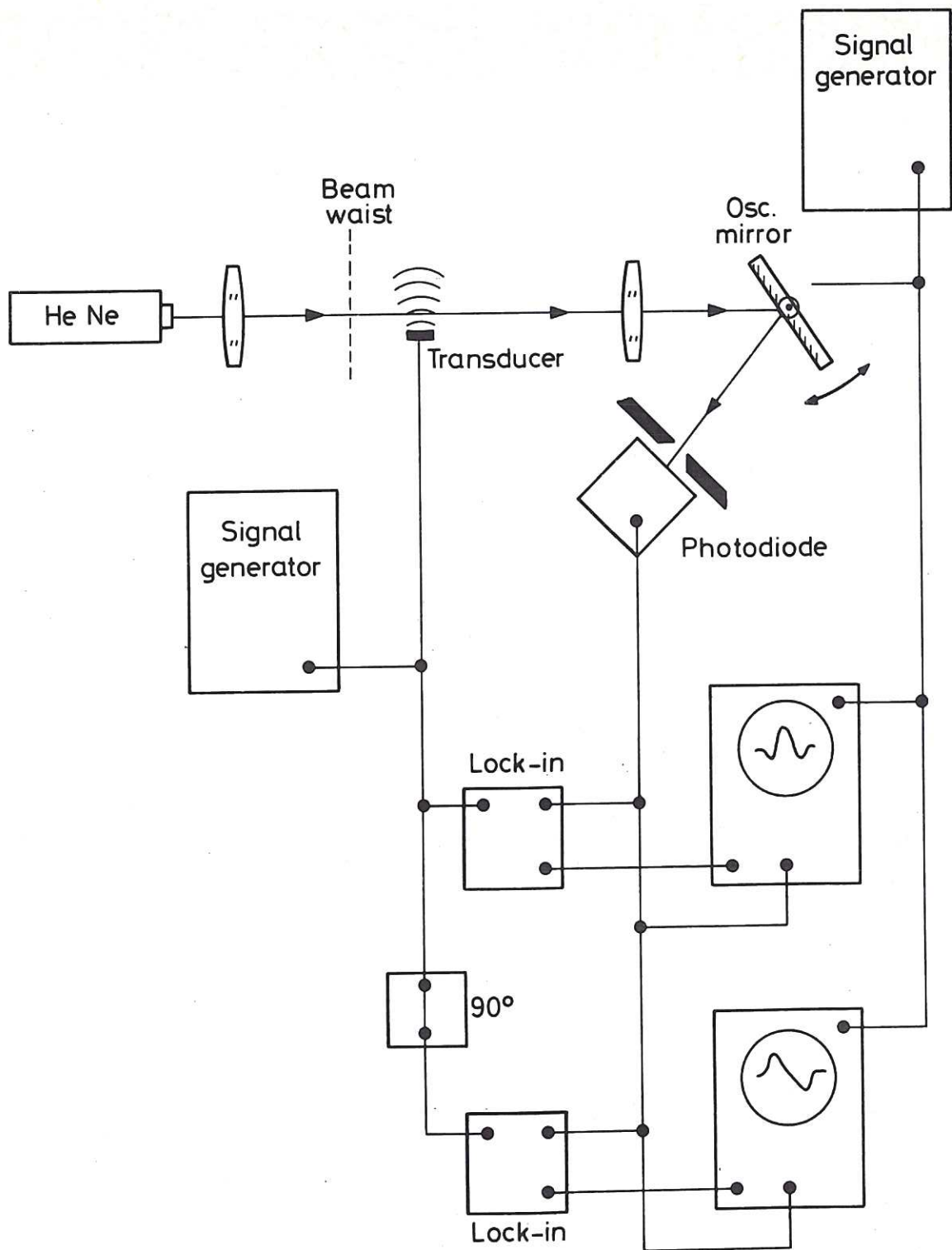


Fig.7 Experimental assembly to measure  $I_{\text{even}}$  and  $I_{\text{odd}}$ .

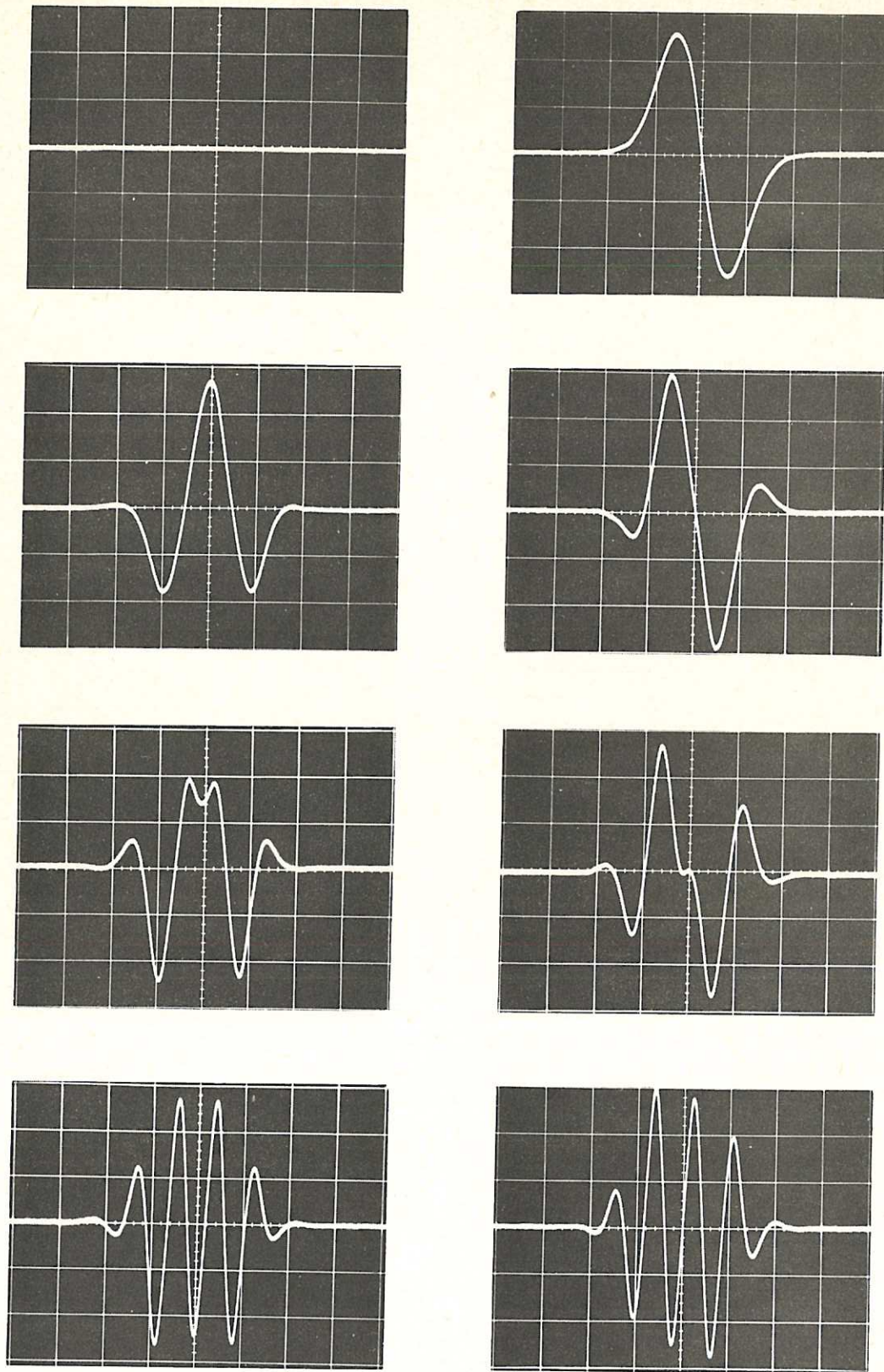


Fig.8 Oscilloscope traces made with the experimental assembly shown in Figure 7. Shown in each case is the diode signal after analysis into  $I_{\text{even}}$  and  $I_{\text{odd}}$  by the lock-in amplifiers.



